A critical role of hydrogen sulfide evolution during MOCVD of single phase thin film tin sulfide using ditertiarybutylsulfide as a less toxic precursor

Andrew J. Clayton[1], Cecile M. E. Charbonneau[2], Peter J. Siderfin[1] and Stuart J. C. Irvine[1]

[1]Centre for Solar Energy Research, College of Engineering, Swansea University, OpTIC, Ffordd William Morgan, St. Asaph Business Park, St. Asaph, Denbighshire, LL17 0JD, UK

[2]Sêr Solar, College of Engineering, Swansea University, Bay Campus, Crymlyn Burrows, Fabian Way, Swansea, West Glamorgan, SA1 8EN, UK

ABSTRACT

Thin film tin sulphide (SnS) was deposited on to molybdenum (Mo) substrates using metal organic chemical vapor deposition at $470^{o}C$ using tetraethyltin and ditertiarybutylsulfide as precursors. In situ mass spectroscopy was used to study the exhaust gas species downstream of the reaction zone. The precursor vapor carrier gas was either nitrogen or hydrogen, thin film SnS only forming when the latter was used. Mass spectroscopy determined that hydrogen sulfide was being produced and playing a critical role in the vapor phase reaction process and adsorption of tin and sulfur on to the Mo surface. As-grown grain sizes were determined by scanning electron microscopy and were observed to be large averaging around 2 microns across. X-ray diffraction showed the films to be single phase SnS without any parasitic Sn_2S_3 or SnS_2 phases, with a small amount of MoS_2 also being detected.

INTRODUCTION

Thin film tin sulfide (SnS) is an attractive material for solar absorption in photovoltaics due to its high absorption coefficient at visible wavelengths [1]. Its earth abundant non-toxic constituents give potential for high throughput module production, which is an important consideration as energy demands increase and materials availability of existing technologies, such as cadmium telluride (CdTe) and copper indium gallium diselenide (CIGS) become uncertain [2]. To date, progress in conversion efficiencies for SnS solar cells has been slow, with a certified world record of 4.4 % [3]. This is very short of the theoretical conversion efficiency limit of 32 % [4]. The challenges with using SnS as a thin film solar cell absorber have mainly been associated to its small grains and poor band alignment with p-n junction counter-parts [3]. This leads to heavy recombination within the bulk material due to grain boundaries acting as recombination centres and poor energy matches to n-type buffers creating losses at the junction.

There are many reports focusing on the appropriate n-type buffer material to create small conduction band offsets with SnS, which has a low electron

affinity [5]. Post-growth annealing steps are generally carried out to enlarge the SnS grains and reduce grain boundary defect concentration [3]. This is typically carried out in a sulfur atmosphere to reduce sulfur loss from the annealed film. Hydrogen sulphide (H_2S) has been shown [3] to be a successful sulfur precursor, also assisting in grain enlargement during post-growth annealing. Unfortunately, H_2S is a highly toxic gas so special measures are required for its use [6]. Ditertiarybutylsulfide (t-Bu_2S) is an alternative sulfur source, with less toxicity than H_2S and has been used by the authors employing the metal organic chemical vapor deposition (MOCVD) process [7]. Tetraethyltin (Et_4Sn) was used in this study as the tin precursor with successful growth of single phase SnS on to molybdenum (Mo) substrates. Post-growth annealing was not necessary with high growth temperatures of 470°C facilitating large grain growth. *In situ* mass spectroscopy was used to give insight into the reaction process.

EXPERIMENT

The MOCVD process used either nitrogen or hydrogen as carry gas to transport the Et_4Sn and t-Bu_2S vapor to the reaction chamber. The Mo substrates were 25 × 75 mm^2 in area and placed on to a heated graphite block with injector position 3 mm above over the upstream region of the substrate. The vapor flow followed a horizontal configuration towards the exhaust. The chamber was kept at atmospheric pressure and the concentration of the precursor vapor was determined by the partial pressure, which was 5.9×10^{-4} and 3.7×10^{-3} atmospheres for Et_4Sn and t-Bu_2S, respectively. It was necessary to use a 6-fold greater concentration of t-Bu_2S to Et_4Sn due to the higher vapor pressure of sulfur compensating for its re-evaporation from the growing SnS film. The authors have reported [7] these optimised parameters in another article.

A Cirrus portable mass spectrometer was used to sample exhaust gas species after the growth chamber to determine by-products produced from the chemical reaction process after SnS film formation. Scanning electron microscopy (SEM) and energy dispersive X-ray spectroscopy (EDX) were carried out with a Hitachi TM3000 bench top instrument and used to assess grain size/shape and approximate stoichiometry of the Sn-S deposits. High resolution (HR)-SEM was carried out with a Hitachi S-4800 instrument equipped with field emission gun (FEG) using beam settings at 2 - 10 keV and 10 µA. X-ray diffraction (XRD) was used with a Phillips X'PERT MPD instrument to determine the thin film crystal structure.

DISCUSSION

It was not possible to obtain thin film SnS when using nitrogen as the carrier gas. This was even the case at chamber temperatures up to 600°C. Thin film SnS only deposited on to the substrates when using hydrogen as carrier gas and at temperatures greater than 410°C.

Thermal decomposition of Et_4Sn

The decomposition products of Et_4Sn, from Et_3Sn to EtSn, with loss of ethyl groups from the precursor, were all detected as soon as Et_4Sn was injected into the chamber using hydrogen as carrier (Figure 1). On heat up, detected concentrations of these by-products increased, correlating with outgassing of sulfur from parasitic wall deposits within the reactor chamber. At a critical temperature between 410 ^{o}C and 420°C, H_2S was detected. The temperature reached a maximum of 470°C with the hydrogen flow

over the substrate. The carrier gas was then switched from hydrogen to nitrogen, resulting in an immediate drop in all detected exhaust gas by-products, even though the chamber temperature increased towards 600°C. This gave two observations, the first being that hydrogen was cooling the substrate surface to a certain degree and secondly that the Et_4Sn thermal decomposition was reliant on hydrogen being used as the carrier gas.
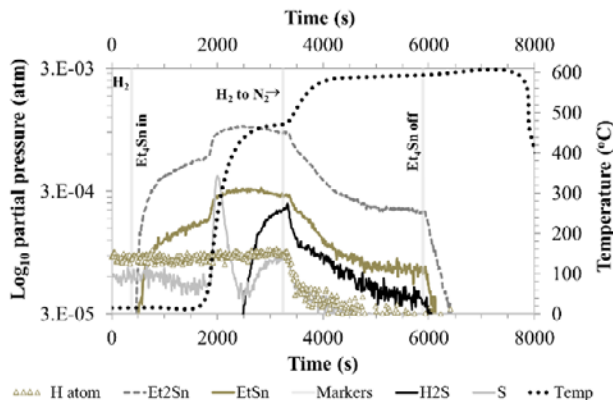

Figure 1. *In situ* mass spectrum of exhaust gas species after Et_4Sn precursor injection as a function of time, temperature and type of carrier gas.

Evolution of H_2S

The initial formation of H_2S during temperature increase with hydrogen flow is attributed by the sulfur release from parasitic wall deposits. Addition of $t-Bu_2S$ results in approximately an order of magnitude increase in the detected partial pressure of H_2S (Figure 2). After $t-Bu_2S$ injection, the sulfur follows a similar trend to H_2S, but at lower partial pressures. The $t-Bu_2S$ decomposition products of $t-Bu-S$ and butane were also detected upon $t-Bu_2S$ injection. When Et_4Sn was then added to the reaction chamber, the detection of both $t-Bu-S$ and butane increased and the butyl group released from $t-Bu_2S$ became detectable, suggesting the Et_4Sn precursor enhanced $t-Bu_2S$ decomposition. Also at the point of Et_4Sn injection, some of the H_2S and sulfur was observed to be consumed. It was determined that this was due to SnS being formed at the substrate surface.
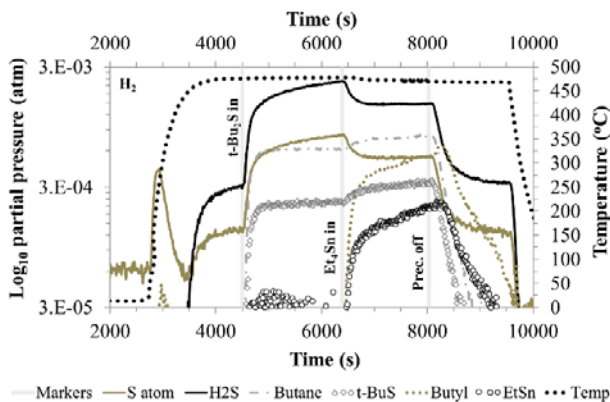
Figure 2. *In situ* mass spectrum of exhaust gas species after t-Bu$_2$S injection followed by Et$_4$Sn precursor injection as a function of time and temperature.

Thin film sns structural properties

XRD showed (Figure 3) the film to have no other Sn-S phases present other than SnS. The dominant peak was that of Mo at 2θ angle of 40.8°. The SnS peaks of the MOCVD-grown thin film correlated with the crystallography open database (COD) patterns for SnS (COD 9008785). There were two preferred orientations in the (101) and (040) planes. A small peak at 2θ angle of 36.5° was present from MoS$_2$, which is known to form from the interaction of sulfur with Mo during deposition [8].
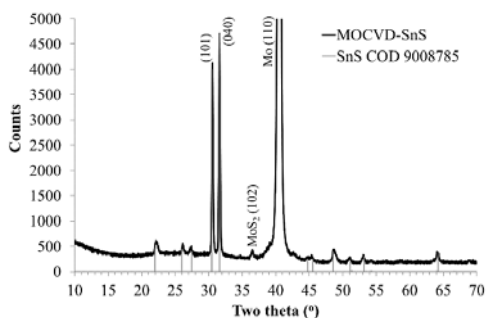

Figure 3. XRD pattern of MOCVD-grown SnS deposited at 470°C on to Mo.

The strong presence of Mo in the XRD pattern suggested the SnS film was thin, or that there was incomplete coverage of the SnS film on the Mo substrate. SEM was carried out on the film to get an indication of grain size (Figure 4). The grains were large, spanning 2 µm across and 4 µm in length in many cases. However, there were areas of

significant contrast which were identified as Mo using EDX. This correlated with the strong peak associated with Mo observed in Figure 3. This signified a large vertical growth rate with incomplete coalescence of the grains. Further growth of the SnS should result in coalescence of the films.
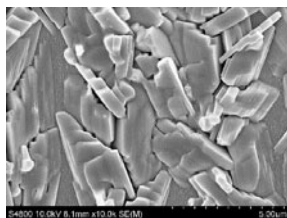

Figure 4. SEM image of MOCVD-grown SnS deposited at 470°C on to Mo.

CONCLUSIONS

XRD determined that single phase thin film SnS was produced using t-Bu$_2$S as a less toxic sulfur precursor alternative to H$_2$S. However, high growth temperatures excessive of 410°C were required to produce SnS with use of hydrogen as carrier gas being essential. This resulted in the formation of H$_2$S within the growth chamber and was determined to be a necessity for Et$_4$Sn and its decomposition products to react and form SnS. Large grains were produced using the as-grown process, but vertical growth rate was high leading to incomplete coalescence of the SnS grains, exposing areas of the Mo substrate. Further growth of the SnS would be expected to lead to coalescence of the grains.

ACKNOWLEDGEMENTS

References

1. M.V. Reddy, G. Sreedevi, P. Chinho, R.W. Miles and K.T.R. Reddy, Curr. Appl. Phys. 15, 588 (2015).
2. C. Candelise, J.F. Speirs and R.J.K. Gross, Renew. Sust. Energy Rev. 15, 4972 (2012).
3. P. Sinsermsuksakul, L. Sun, S.W. Lee, H.H. Park, S.B. Kim, C. Yang and R.G. Gordon, Adv. Energy Mater. 1400496 (2014).
4. S. Siebentritt, Sol. Energy Mater. Sol. Cells, 95, 1471 (2011).
5. L.A. Burton, Y. Kumagai, A. Walsh and F. Oba, J. Mater. Chem. A, 5, 9132 (2017).
6. Z. Jianwen, L. Da and F. Wenxing, Proc. Eng. 26, 1878 (2011).
7. A.J. Clayton, C.M.E. Charbonneau, W.C. Tsoi, P.J. Siderfin and S.J.C. Irvine, Sci. Tech. Adv. Mater. Accepted for publication, DOI: 10.1080/14686996.2018.1428478.
8. W. Li, J. Chen, H. Cui, F. Liu and X. Hao, Mater. Lett. 134, 87 (2014).